

INFILTRATION THROUGH VARIABLY SATURATED SOIL

A Thesis

Presented to the

Faculty of

California State University, Fullerton

In Partial Fulfillment

of the Requirements for the Degree

Master of Science

in

Civil Engineering

By

Jose L. Aviña

Thesis Committee Approval:

Dr. Phoolendra Mishra, Department of Civil & Environmental Engineering

Dr. Garrett Struckhoff, Department of Civil & Environmental Engineering

Dr. Jeff Kuo, Department of Civil & Environmental Engineering

Spring, 2016

ABSTRACT

Infiltration is an important aspect to the hydrologic cycle as it allows for groundwater recharge. In California especially, groundwater is used for agriculture, industrial usage, and as drinking water. This Thesis presents an analytical model for time dependent infiltration through a variably saturated soil. Water is considered to begin infiltrating soil at the ground surface and moves through the vadose zone towards the datum of the system (the water table) where pressure head is constrained to zero. The developed model calculates important soil characteristic parameters such as hydraulic conductivity, K , water content, θ , and pressure head, ψ , as a function of depth. The solution introduces four parameters (a_k, ψ_k, a_c , and ψ_a) to represent K and θ as exponential functions. The proposed model is then compared to existing exponential function solutions for various times. The comparison illustrates the versatility of using a four parameter exponential representation for infiltration. Furthermore, the proposed solution is validated against the numerical solution of HYDRUS-1D, which employs the widely used van Genuchten-Mualem constitutive model. Additionally, once parameters a_k and ψ_k are known, one can obtain van Genuchten parameters α and n . Finally, the constitutive exponential expressions for hydraulic conductivity and water content are compared to the van Genuchten-Mualem expressions.

TABLE OF CONTENTS

ABSTRACT	II
LIST OF FIGURES	V
LIST OF TABLES	VI
ACKNOWLEDGMENTS	VII
1 BACKGROUND AND MOTIVATION	1
1.1 Introduction	1
1.2 Darcy's Law (1856)	3
1.3 Green-Ampt Model (1911)	5
1.4 Horton's Model (1930s)	8
1.5 Philips Equation (1957)	9
1.6 Richards' Equation (1931)	10
1.7 Motivation	11
2 INFILTRATION TOWARDS THE WATER TABLE	13
2.1 Overview	13
2.2 Statement of Problem	13
2.3 Linearization of Richards' equation	16
2.4 Laplace Transformation	17
2.5 Single Layer Homogeneous Soil	18

2.5.1	Particular Solution	21
2.5.2	General Solution	21
2.5.3	Unique Solution	22
3	RESULTS AND DISCUSSION	27
3.1	Introduction	27
3.2	Comparison with Analytical Solution	27
3.2.1	Laplace inversion using software program	29
3.2.2	Graphical comparison	29
3.3	Comparison with Numerical Solution	32
3.4	Determining van Genuchten Parameters and Comparison of Exponential Functions	34
4	CONCLUSION AND FUTURE SCOPE	37
4.1	Conclusion	37
4.2	Future Scope	38
	APPENDIX : HYDRUS-1D AND FITTED MODEL OUTPUTS	40
	BIBLIOGRAPHY	47

LIST OF FIGURES

Figure	Page
1.1 Hydrologic Cycle	2
1.2 Schematic representation of Darcy's Law	4
1.3 Comparison of Modified Green-Ampt Models with Original Green-Ampt Model(Ma et al. (2010))	7
2.1 Schematic representation of system	14
3.1 Wetting front: depth versus pressure head for $\psi_k = \psi_a = 1 \text{ cm}$, $a_k = 0.05 \text{ cm}^{-1}$ $a_c = 0.04 \text{ cm}^{-1}$ and $\alpha = 0.05 \text{ cm}^{-1}$	28
3.2 Drainage: depth versus pressure head for $\psi_k = \psi_a = 1 \text{ cm}$, $a_k = 0.035 \text{ cm}^{-1}$ $a_c = 0.025 \text{ cm}^{-1}$ and $\alpha = 0.035 \text{ cm}^{-1}$	30
3.3 Depth versus water content for $\psi_k = \psi_a = 1 \text{ cm}$, $a_k = 0.06 \text{ cm}$ $a_c = 0.05 \text{ cm}$ and $\alpha = 0.06 \text{ cm}^{-1}$	31
3.4 Depth versus hydraulic conductivity at $t = 50 \text{ hrs}$ when $\psi_k = \psi_a = 1 \text{ cm}^{-1}$	32
3.5 Depth versus hydraulic conductivity at $t = 50 \text{ hrs}$ when $\psi_k = \psi_a = 1 \text{ cm}^{-1}$	33
3.6 Depth versus pressure head for $t = 50 \text{ hrs}$ when $\psi_k = 5.4626 \text{ cm}$, $\psi_a = 9 \text{ cm}$, $a_k = 0.135 \text{ cm}^{-1}$, $a_c = 0.029 \text{ cm}^{-1}$, $\alpha = 0.0416 \text{ cm}^{-1}$, and $n = 2.4963$	34
3.7 Depth versus pressure head for $\psi_k = 5.4626 \text{ cm}$, $\psi_a = 9.0 \text{ cm}$, $a_k = 0.135 \text{ cm}^{-1}$, $a_c = 0.029 \text{ cm}^{-1}$, $\alpha = 0.0416 \text{ cm}^{-1}$, and $n = 2.4963$	35

LIST OF TABLES

<u>Table</u>		<u>Page</u>
3.1	Soil characteristics for Figures 3.1, 3.2, 3.3	28
3.2	Soil characteristics for Figures 3.5 and 3.4	28
3.3	Soil characteristic inputs for HYDRUS-1D software	33
A.1	HYDRUS-1D Simulated Data	40
A.2	MATLAB Data	44

ACKNOWLEDGMENTS

Firstly, I would like to thank my advisor Dr. Phoolendra Mishra for his never ending support throughout this work and my time in graduate school. His dedication and enthusiasm to his profession and for his students is unparalleled and serves as an inspiration. He has believed in me and propelled me to accomplish academic milestones I had only dreamed of. I am forever grateful for his mentorship both professionally and personally. I could not have asked for a better advisor, mentor, and teacher.

I would also like to thank my committee members Dr. Garrett Struckhoff and Dr. Jeff Kuo for their support. Dr. Struckhoff has always provided insights towards conducting research and being thorough with experiments. For that I am greatly appreciative. Dr. Kuo has been a tremendous proponent of mine throughout my studies. I thank him for his professional advice and the wisdom he has shared with me. Without their advocacy this thesis would not be made possible.

Words cannot express the appreciation I have for my parents. Without their sacrifices and support I would not have accomplished my dream of attaining my master's degree. I also want to thank Elizabeth for being by my side throughout the years, consistently pushing me to strive for higher goals. Finally, thank you to my siblings for holding me to a high standard and showing me how to become a responsible adult.

DEDICATION

My parents

CHAPTER 1

BACKGROUND AND MOTIVATION

1.1 INTRODUCTION

In recent years the air-water-soil interaction in the vadose zone has become an area of interest for several fields of engineering. Geotechnical engineers may be interested in water content or void ratio to estimate strength of soil, settlement, or for erosion control. Environmental engineers require groundwater speeds to mitigate contaminant migration. Water resource engineers must account for groundwater recharge into an aquifer to analyze water supply. Interest unsaturated soil flow modeling continues to grow due to the importance it has on the water cycle, seen in Figure 1.1. Infiltrated water is the source of nourishment for trees and other vegetation and can even be consumed by humans once it is pumped using extraction wells. As important as it is to understand groundwater flow, scientists and engineers have been attempting to discover its true nature since 1911.

Before we delve into infiltration models let us consider key parameters and their significance. Water content, θ , is a common variable in infiltration models. It describes the amount of water in soil per volume of soil. Values for θ are fairly easy to obtain from soil samples by calculating the in-situ weight of soil and comparing it to the dry weight of the same soil sample. Being measured as a ratio of volumes, θ is unitless and often expressed as a percentage. Infiltration models usually consider

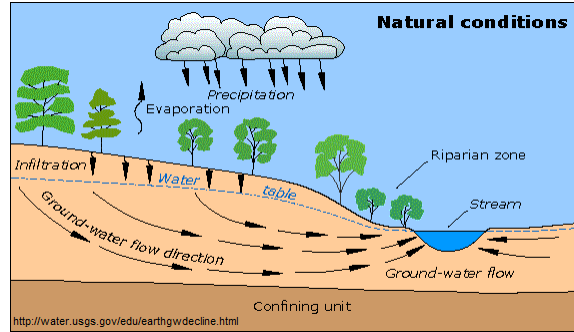


FIGURE 1.1: Hydrologic Cycle

θ to be constant with respect to time or location. However, θ can in fact change with both time and location as will be discussed in the following chapter. Two parameters often used in infiltration models are residual water content, θ_r and saturated water content, θ_s . The former, which has no physical importance, is defined as the water content for which the gradient $\frac{d\theta}{dh} = 0$ and the latter is identical to porosity due to void space being occupied only by water.

In hydrological science water potential is universally measured in terms of head, h , having units of length. Head combines gravitational potential head, elevation potential head, and kinematic potential head. However, kinematic potential head is neglected for the case of groundwater flow due to insignificant contribution in head because of slow velocities.

Another important parameter for infiltration of any subsurface modeling is hydraulic conductivity, K . Hydraulic conductivity is a parameter which describes the rate at which water flows through a porous media, usually soil. K has units of length per time, such as $\frac{ft}{min}$ or $\frac{m}{s}$. Whether infiltration models are empirical or theoretical, we clearly see the need to incorporate hydraulic conductivity as it describes speed of water. While K is obtained empirically through a variety of field tests and is assumed to be homogeneous and isotropic throughout the system,

hydraulic conductivity is itself a function of water and soil properties such as hydraulic head, h .

With the frequently used infiltration parameters having been discussed, let's delve into what infiltration describes. Infiltration is the process by which water on the ground surface enters the soil where f is infiltration rate. The potential infiltration rate would be the rate of infiltration when water is ponded at soil surface. In case of no ponding, the actual rate of infiltration would be smaller than the potential infiltration rate. Cumulative infiltration is accumulated depth of water infiltrated in soil and generally expressed as,

$$F(t) = \int_0^t f(\tau) d\tau. \quad (1.1)$$

In ideal conditions of isotropic, heterogeneous soil characteristics and at constant rainfall, water infiltrates the soil surface and continues downward. Assuming initially dry soil, water infiltration creates a wetting front as it travels deeper into the soil, saturating it. Once the top soil is saturated, runoff or ponding can occur and infiltration rate decreases. This process is explored and modeled in the following subsections beginning with the fundamental Darcy's law and looking at how infiltration modeling has evolved through time.

1.2 DARCY'S LAW (1856)

In 1856, Darcy (1856) studied the behavior of flowing water by comparing it to the principal of heat conduction (Fourier's law), diffusion theory (Fick's law), and Ohm's law and applied this to water flow through porous media. Through

experimentation Darcy found the flux of water through a porous media to be described as,

$$q = -K \frac{\partial h}{\partial z} \quad (1.2)$$

where q describes the discharge per unit area having units of $\frac{\text{length}}{\text{time}}$. Figure 1.2 describes a laboratory setup for the Darcy experiment.

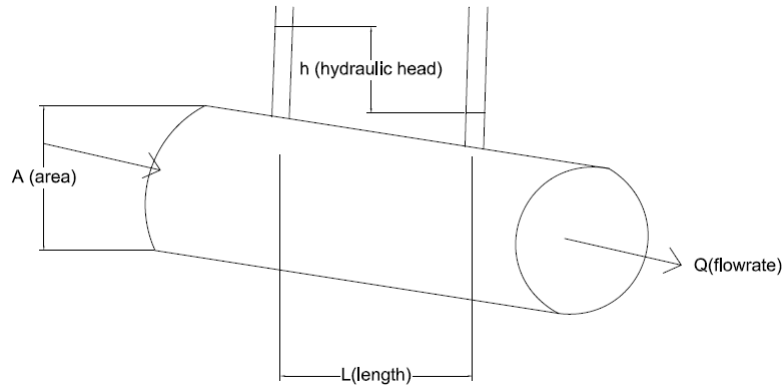


FIGURE 1.2: Schematic representation of Darcy's Law

Darcy's law only scratches the surface of the intricate nature that is water flow in porous media. While its uses are far reaching in groundwater flow modeling Darcy's law simplifies the physical phenomenon by assuming constant hydraulic conductivity. In practice, K is a function of water content and the effects of hysteresis should be considered as well. An important note is the applicability of Darcy's law to saturated soils where the effects of air water pressure interaction can be neglected. Additionally, Darcy's law is limited to laminar flow conditions such as flow in fine grained soils but fails to accurately describe water movement in coarse grained soils due to turbulent flow.

1.3 GREEN-AMPT MODEL (1911)

The Green and Ampt (1911) method of infiltration estimation is derived from Darcy's law but considers many variables previously ignored. The Green-Ampt equation, below, describes hydraulic conductivity, K , as a function of time and water infiltrated during the elapsed time.

$$\int_0^{F(t)} \frac{F}{F + \psi\Delta\theta} dF = \int_0^t K dt \quad (1.3)$$

where ψ is wetting front soil suction head, θ is water content, and F is cumulative volume infiltrated at time t . Integrating equation (1.3) yields,

$$F(t) = Kt + \psi\Delta\theta \ln\left[1 + \frac{F(t)}{\psi\Delta\theta}\right] \quad (1.4)$$

It is plain to see equation (1.4) is an iterated function, one must first make an initial guess for F at t and hope for convergence. This can lead to complications if initial guesses are too different than the actual values.

Taking the derivative of (1.4) gives the infiltration rate at time t ,

$$f(t) = K\left[\frac{\psi\Delta\theta}{F(t)} + 1\right] \quad (1.5)$$

where the parameters follow those of the cumulative infiltration function.

The Green-Ampt model assumes a ponded surface, meaning the actual rate of infiltration is equal to the infiltration capacity at all times. However, this is not

always the case, such as early storm events when water is beginning to enter the soil and the rate of infiltration has not yet reached infiltration capacity. Mein and Larso (1973) proposed a modification to the Green-Ampt model to account for two cases of rainfall intensity. The first case proposes that runoff never occurs when the rainfall intensity is less than saturated conductivity of soil. In this case, no infiltration volume is calculated. Once the rainfall intensity is greater than the saturated soil conductivity the Green-Ampt equation is employed to calculate the cumulative infiltration volume. Modeling software such as Storm Water Management Model (SWMM) compares rainfall intensity i and saturated soil conductivity K_s using the two stage method to estimate infiltration.

Almedeij and Esen (2013) further explored the work of Mein and Larso (1973) saying their modification underestimates cumulative infiltration, F but can be improved. Their study suggests increasing the time to ponding in the Green-Ampt equation to indicate the time when cumulative infiltration potential of the soil is fully saturated. Using five soil types and five different rainfall rates for each soil, Almedeij and Esen (2013) compared the classic Green-Ampt equation with the Mein-Larson method and the proposed ponding time change. It is important to note that the proposed modification only affects the first stage of the Mein-Larson method and the second stage remains unchanged. The cumulative infiltration of each soil was calculated using the three methods and the results showed the classic Green-Ampt equation and the Almedeij and Esen (2013) modification closely matched, whereas the Mein-Larson method underestimated F .

In its original capacity, the Green-Ampt equation assumes the wetted zone is fully saturated and therefore does not account for air entrapment. Recently, Ma et al. (2010) introduced a saturation coefficient, S_a , for the Green-Ampt model to account

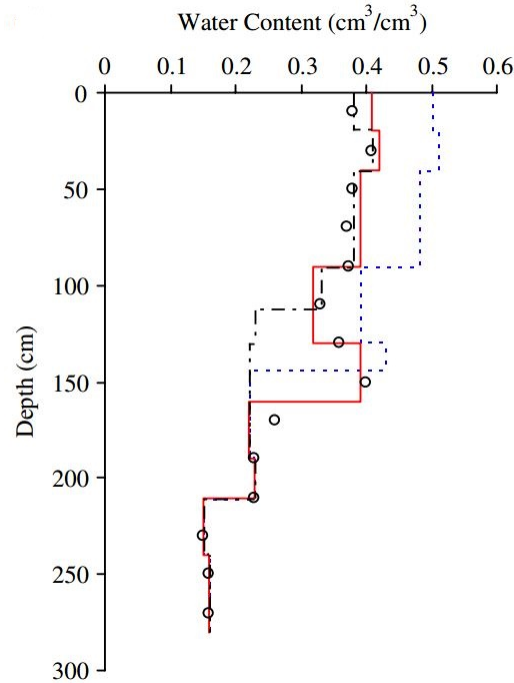


FIGURE 1.3: Comparison of Modified Green-Ampt Models with Original Green-Ampt Model(Ma et al. (2010))

for air entrapment. They define this coefficient as $S_a = 1 - \frac{\theta_r}{\theta_s}$ where θ_s is the saturated volumetric water content and θ_r is the addition of the residual air and water contents, $\theta_{ra} + \theta_{rw}$. For their modification to the Green-Ampt equation, S_a is multiplied to θ and K so, $\theta_a = S_a\theta_s$ and $K_a = S_aK_s$ are the actual water content and hydraulic conductivity, respectively. Ma et al. (2010) ran infiltration experiments in laboratory and field conditions to verify the validity of their model as well as the original Green-Ampt equation and a modified version presented by Bouwer (1966). The modification accounting for air entrapment proved promising as their simulations closely resembled both experiments better than the Bouwer model and the original Green-Ampt equation. Figure 1.3 illustrates the usefulness of including air entrapment. It describes how water content changes with depth where the soil surface is set to 0. It is clear to see that the model closely resembles

the observed data for the elapsed time of 2,580 minutes shown in Figure 1.3.

Given the parameters of equations (1.3) and (1.4), obtaining a numerical solution is only a matter of trial and error with initial guesses for F . The age of technology encourages the use of the Green-Ampt equation due to highly efficient computing powers. However, the underlying assumption of uniform and constant K is invalid for most cases, especially when considering a time frame beginning just before a storm event and ending during the storm event or after rainfall has stopped.

1.4 HORTON'S MODEL (1930S)

Horton (1933) gave a simplified empirical formula saying infiltration starts at a constant rate, f_0 , and is decreasing exponentially with time, t . After some time when the soil saturation level reaches a certain value, the rate of infiltration will level off to the rate f_c . Horton's equation is given by

$$f(t) = f_c + (f_0 - f_c) e^{-kt} \quad (1.6)$$

where k is the rate of decrease in infiltration capacity and f , with units of $\frac{\text{depth}}{\text{time}}$ is the infiltration capacity at time t . Differentiating Horton's model gives us the cumulative infiltration at a given time and is as follows

$$F(t) = f_c t_p + \frac{f_0 - f_c}{k} (1 - e^{-kt_p}) . \quad (1.7)$$

In this equation, t_p is the equivalent time for the actual infiltrated volume to equal the volume under the infiltration capacity curve. When each parameter of these equations are known the model does a fairly good job of describing infiltration.

However, obtaining the values of k and f_0 are difficult, making the equations rather inconvenient.

1.5 PHILIPS EQUATION (1957)

John R. Philip published a series of articles titled *The Theory of Infiltration*. In *The Theory of Infiltration:6 Effect of Water Depth Over Soil* (Philip, 1958) Philip derives an infiltration equation from Richards Equation for the case of infiltration into a homogeneous semi-infinite medium with initial moisture content θ_0 and water depth h . After some mathematical manipulation and rearranging of the formula we reach Philips Equations for infiltration rate and cumulative infiltration, respectively,

$$f(t) = \frac{1}{2}St^{-1/2} + K \quad (1.8)$$

and

$$F(t) = St^{1/2} + Kt. \quad (1.9)$$

In equations (1.8) and (1.9) S represents sorptivity, an empirical parameter and a function of soil suction potential. Additionally, K and t are the familiar parameters of hydraulic conductivity and time, respectively. These equations are simple forms of the power series in which Philip originally published his work. It is worth noting Philips Equations assume a saturated hydraulic conductivity value.

1.6 RICHARDS' EQUATION (1931)

Lorenzo Richards worked on improving the Darcy-Buckingham equation which describes water movement in unsaturated soils. In his work, he developed a non-linear partial differential equation to represent the movement of water in unsaturated soils (Richards, 1931). Richards equation is as follows,

$$\frac{\partial \theta}{\partial t} = \frac{\partial}{\partial z} [K(\theta) \left(\frac{\partial \psi}{\partial z} + 1 \right)] \quad (1.10)$$

where θ is water content, ψ is pressure head, K is hydraulic conductivity as a function of θ . Here, the influence θ has on hydraulic conductivity is incorporated into the equation whereas Darcy's law and the Green-Ampt model, in its original form, assume a constant value of K . Richards' equation encompasses the system as a whole because it accounts for conditions varying in time and depth, such as θ , K , and ψ . Herrada et al. (2014) explored improvements of the Richards equation to simulate infiltration during unsteady rainfall events as well as ponding and non-ponding conditions and varying initial water distributions. This numerical method uses the finite volume scheme to model infiltration behavior under conditions described previously. Results from this approach closely followed the true nature of infiltration, illustrating the pertinent use of Richards equation.

One of the most cited applications of Richards' equation comes from the Van Genuchten (1980)-Mualem (1976) constitutive model, expressed as (1.11) and (1.12). Infiltration modeling software, such as HYDRUS and SWIMv1/SWIMv2, simulate water flow through unsaturated soil by utilizing the van Genuchten-Mualem model.

$$S_e(\psi) = \frac{\theta(\psi) - \theta_r}{\theta_s - \theta_r} = \frac{1}{(1 + |\alpha\psi|^n)^m} \quad (1.11)$$

$$K(\theta) = K_s S_e^l \left[1 - \left(1 - S_e \left(\frac{1}{m} \right) \right)^m \right]^2 \quad (1.12)$$

and

$$m = 1 - \frac{1}{n} \quad (1.13)$$

where S_e is effective water content, l is pore-connectivity parameter (usually set to 0.5), ψ is pressure head, and θ_s and θ_r are saturated and residual water content, respectively. Parameters m , n , and α are empirical and must be solved for through experimentation. Sometimes solving for m , n , and α can be too cumbersome, increasing the need for parameter estimation techniques. This thesis will present a method to determine these parameters after establishing an analytical solution to a system of unsaturated soil exhibiting time dependent infiltration.

1.7 MOTIVATION

Srivastava and Yeh (1991) validated the use of Richard's equation for representing water infiltration in the vadose zone. They use a single exponential decay parameter, α , in describing hydraulic conductivity and water content. However, in some cases, α is insufficient to describe soil characteristics when the soil exhibits a mixture of K and θ . Mishra and Neuman (2010) presented a four parameter constitutive solution for water flow during well pumping. Their results strongly

indicated using a_k , a_c , ψ_k , and ψ_a as exponential parameters and pressure head values to better represent soil characteristics, respectively.

This thesis develops a four parameter constitutive model by representing hydraulic conductivity and water content as exponential functions using a_k , a_c , ψ_k , and ψ_a , similar to Mishra and Neuman (2010). The solution is compared to that of Srivastava and Yeh for the effects of varying parameters a_k and a_c . Next, the developed solution is validated against the HYDRUS-1D numerical solution obtained using the Van Genuchten (1980)-Mualem (1976) model. Furthermore, using the relationship given by Ghezzehei et al. (2007) with ψ_k and a_k one can predict van Genuchten parameters α and n .

CHAPTER 2

INFILTRATION TOWARDS THE WATER TABLE

2.1 OVERVIEW

This chapter presents an analytical solution for one-dimensional infiltration through variably saturated soil towards the water table. Primarily following and improving on the work of Srivastava and Yeh (1991) by introducing new parameters to allow for more flexibility in representing variably saturated soil. The Srivastava and Yeh solution also considers one-dimensional infiltration and uses exponential functions to represent water content, θ , and hydraulic conductivity, K . Both solutions consider time dependent flux from the ground towards the water table and are also functions of depth, z . This chapter introduces a system for infiltration including boundary and initial conditions required to develop a solution using a four parameter approach similar to Mishra and Neuman (2011). Finally, this chapter establishes an analytical solution in Laplace space for non-dimensional hydraulic conductivity, k .

2.2 STATEMENT OF PROBLEM

In the previous chapter, several infiltration models were discussed where their solutions are fundamentally physical or numerical such as Horton's model or the

Srivastava and Yeh solution, respectively. This chapter relies on four parameters (a_k, a_c, ψ_k, ψ_a) with little physical meaning but enable for an expanded representation of soil characteristics. Both a_k and a_c are exponential decay parameters used to describe k and θ , respectively. The parameter a_k is analogous to α used by Srivastava and Yeh (1991) and α used in the Van Genuchten (1980)-Mualem (1976) constitutive model.

Srivastava and Yeh (1991) developed an analytical solution for downward infiltration to the water table through variably saturated soil. Similarly, this chapter considers one-dimensional infiltration towards the water table, located L distance below the ground as in Figure 2.1. Additionally, as initial conditions for time $t \leq 0$, flux from the ground is q_A and for time $t > 0$ flux becomes q_B . Allowing for change in infiltration rates results in a variety of system conditions. For example, the beginning of a rain event can have $q_A = 0 \frac{cm}{hr}$ then increase to $q_B = 0.5 \frac{cm}{hr}$. Similarly, for the end of a rain event $q_A = 0.5 \frac{cm}{hr}$ can decrease to $q_B = 0 \frac{cm}{hr}$.

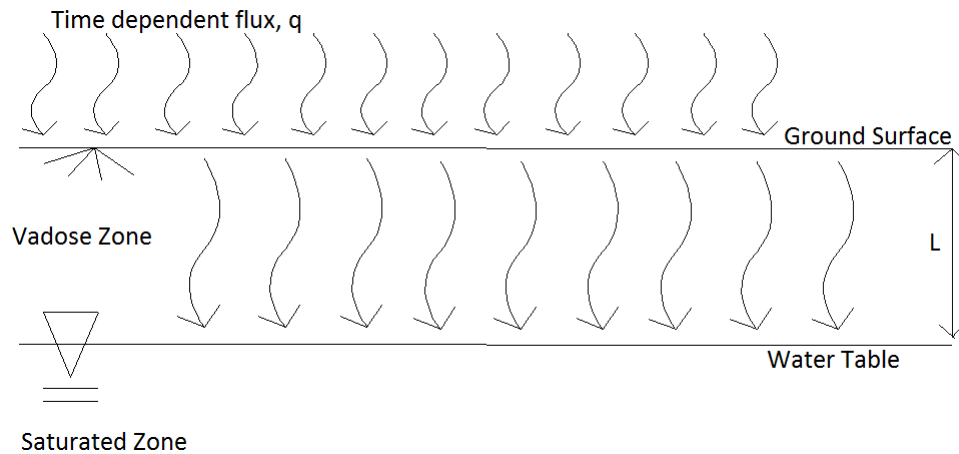


FIGURE 2.1: Schematic representation of system

The flow in unsaturated zone is governed by Richards' equation

$$K \frac{\partial}{\partial z} \left[k(\psi) \frac{\partial(\psi + z)}{\partial z} \right] = \frac{\partial \theta}{\partial t} = C(\psi) \frac{\partial \psi}{\partial t} \quad (2.1)$$

subject to an initial pressure distribution corresponding to the steady state for a prescribed initial flux (q_0) at the surface and constant head boundary at water table

$$\frac{\partial h}{\partial z} = \frac{q_0}{K} \quad (2.2)$$

where K is saturated hydraulic conductivity, $0 \leq k(\psi) \leq 1$ is relative (ratio of actual to saturated) hydraulic conductivity. $C(\psi) \geq 0$ is specific moisture capacity defined as $C(\psi) = d\theta/d\psi$ and θ is volumetric water content.

Following Mishra and Neuman (2010), we represent water retention and relative hydraulic conductivity characteristics by means of Gardner (1958) type exponential functions

$$S_e = \frac{\theta(\psi) - \theta_r}{\theta_s - \theta_r} = e^{a_c(\psi - \psi_a)} \quad (2.3)$$

$$k(\psi) = e^{a_k(\psi - \psi_k)} \quad (2.4)$$

where S_e is effective saturation, θ_r and θ_s are residual and saturated water content, respectively. Exponential decay parameters a_k and ψ_k may differ from a_c and ψ_a in (2.3). For the case in which $a_c = a_k$, the solution reduces to that of Srivastava and Yeh (1991).

The parameter ψ_k represents a pressure head above which relative hydraulic conductivity is effectively equal to unity. In some cases ψ_k can equal ψ_a (air entry pressure) but that is not always the case. When $\psi_k \neq \psi_a$ a four parameter constitutive model can be employed as discussed in Mishra and Neuman (2010) and provides the starting point for the next section.

2.3 LINEARIZATION OF RICHARDS' EQUATION

Taking derivative of $\theta(\psi)$ and $k(\psi)$ with respect to ψ gives,

$$\frac{\partial\theta(\psi)}{\partial\psi} = (\theta_s - \theta_r) a_c e^{a_c(\psi-\psi_a)} \quad (2.5)$$

and

$$\frac{\partial k(\psi)}{\partial\psi} = a_k e^{a_k(\psi-\psi_k)} \quad (2.6)$$

therefore,

$$\frac{\partial\theta(\psi)}{\partial k(\psi)} = (\theta_s - \theta_r) \frac{a_c}{a_k} e^{(a_k\psi_k - a_c\psi_a)} e^{(a_c - a_k)\psi} \quad (2.7)$$

Rearranging $k(\psi)$ function gives

$$\psi = \frac{1}{a_k} \ln(k(\psi)) + \psi_k \quad (2.8)$$

Therefore,

$$\frac{\partial\psi}{\partial z} = \frac{1}{a_k} \frac{1}{k(\psi)} \frac{\partial k(\psi)}{\partial z} \quad (2.9)$$

Expanding Richards' equation gives,

$$K \frac{\partial}{\partial z} \left[k(\psi) \frac{\partial\psi}{\partial z} + k(\psi) \right] = \frac{\partial\theta(\psi)}{\partial k(\psi)} \frac{\partial k(\psi)}{\partial t} \quad (2.10)$$

Substituting derivatives gives,

$$\frac{K}{a_k} \left[\frac{\partial^2 k(\psi)}{\partial z^2} + a_k \frac{\partial k(\psi)}{\partial z} \right] = (\theta_s - \theta_r) \frac{a_c}{a_k} e^{(a_k \psi_k - a_c \psi_a)} e^{(a_c - a_k) \psi} \frac{\partial k(\psi)}{\partial t} \quad (2.11)$$

which upon rearranging becomes

$$\frac{\partial^2 k(\psi)}{\partial z^2} + a_k \frac{\partial k(\psi)}{\partial z} = \frac{a_c (\theta_s - \theta_r)}{K} \frac{e^{a_k \psi_k}}{e^{a_c \psi_a}} e^{(a_c - a_k) \psi} \frac{\partial k(\psi)}{\partial t} \quad (2.12)$$

2.4 LAPLACE TRANSFORMATION

Similar to Srivastava and Yeh (1991), dimensionless parameters are introduced and the Laplace transformation is taken on the dimensionless equation. The following sections makes use of the following dimensionless parameters:

$$z_D = z a_k \quad (2.13)$$

which leads to

$$L_D = L a_k \quad (2.14)$$

$$t_s = \frac{a_c K t}{(\theta_s - \theta_r)} \quad (2.15)$$

Substituting the dimensionless parameters into (2.12) gives

$$\frac{\partial^2 k(\psi)}{\partial \left(\frac{z_D}{a_k}\right)^2} + a_k \frac{\partial k(\psi)}{\partial \left(\frac{z_D}{a_k}\right)} = a_c \frac{(\theta_s - \theta_r)}{K} \frac{e^{a_k \psi_k}}{e^{a_c \psi_a}} e^{(a_c - a_k) \psi} \frac{\partial k(\psi)}{\partial \left(\frac{t_s (\theta_s - \theta_r)}{a_c K}\right)} \quad (2.16)$$

Canceling some variables and rearranging (2.16) simplifies to the dimensionless equation

$$a_k^2 \frac{\partial^2 k(\psi)}{\partial z_D^2} + a_k^2 \frac{\partial k(\psi)}{\partial z_D} = a_c^2 \frac{e^{a_k \psi_k}}{e^{a_c \psi_a}} e^{(a_c - a_k) \psi} \frac{\partial k(\psi)}{\partial t_s} \quad (2.17)$$

Dividing the equation by a_k^2 gives

$$\frac{\partial^2 k(\psi)}{\partial z_D^2} + \frac{\partial k(\psi)}{\partial z_D} = \left(\frac{a_c}{a_k} \right)^2 \frac{e^{a_k \psi_k}}{e^{a_c \psi_a}} e^{(a_c - a_k) \psi} \frac{\partial k(\psi)}{\partial t_s} \quad (2.18)$$

Now letting $c = \left(\frac{a_c}{a_k} \right)^2 \frac{e^{a_k \psi_k}}{e^{a_c \psi_a}}$, and $\lambda = -\left(\frac{a_c}{a_k} - 1 \right)$ by replacing ψ with $-\frac{z_D}{a_k}$, (2.18)

becomes

$$\frac{\partial^2 k(\psi)}{\partial z_D^2} + \frac{\partial k(\psi)}{\partial z_D} = ce^{\lambda z_D} \frac{\partial k(\psi)}{\partial t_s} \quad (2.19)$$

Taking the Laplace Transform of (2.19) and rearranging gives

$$\frac{\partial^2 \bar{k}}{\partial z_D^2} + \frac{\partial \bar{k}}{\partial z_D} = ce^{\lambda z_D} (p\bar{k} - k_0) \quad (2.20)$$

where the transformation occurs of k by \bar{k} and p is the Laplace parameter.

Rearranging again we reach

$$\frac{\partial^2 \bar{k}}{\partial z_D^2} + \frac{\partial \bar{k}}{\partial z_D} - ce^{\lambda z_D} p\bar{k} + ce^{\lambda z_D} k_0 = 0 \quad (2.21)$$

Equation (2.21) is the governing equation for the system discussed and will be referred to as such from hereafter. To achieve a particular and general solution to (2.21) a single layer of homogeneous soil constrained to a set of initial and boundary conditions will be explored in the following sections.

2.5 SINGLE LAYER HOMOGENEOUS SOIL

Vertical infiltration into a homogeneous single layer of soil is explored. Water infiltrates the ground surface towards the water table where $z = 0$ as shown in Figure 2.1. Total length of infiltration, $\Delta z = L$, is the depth from the ground surface to the water table. Pressure at the water table is set to $\psi_0 = 0$ and q_A is the initial flux through the soil surface. For times $t > 0$ the constant flux through the soil surface is q_B . In our system, z is positive upward from the water table to the ground surface.

From the above description of the system, the following relationship is observed for $\psi = \psi_0 = 0$ at $z = 0$. Applying this to (2.4) the following is obtained

$$k(0, t) = e^{-a_k \psi_k} \quad (2.22)$$

Now consider Darcy's relationship

$$q = k \frac{\partial h}{\partial z} \quad (2.23)$$

where q is a dimensionless flux due to k being defined as a ratio quantity described in Chapter 2 Section 1.1 and $\frac{\partial h}{\partial z}$ also being dimensionless. Next, (2.23) is rearranged as

$$q = k \left(\frac{\partial \psi}{\partial z} + 1 \right) \quad (2.24)$$

because $h = z + \psi$ and $\frac{\partial h}{\partial z} = \frac{\partial \psi}{\partial z} + 1$. Therefore, replacing $\frac{\partial \psi}{\partial z}$ with $\frac{1}{a_k k} \frac{\partial k}{\partial z}$

$$q = k \left(\frac{1}{a_k k} \frac{\partial k}{\partial z} + 1 \right) \quad (2.25)$$

$$q = \frac{1}{a_k k} \frac{\partial k}{\partial z} + k \quad (2.26)$$

and from the dimensionless parameter $z_D = z a_k$

$$q = \frac{\partial k}{\partial z_D} + k \quad (2.27)$$

From the boundary condition, at $z = L$ for $t > 0$

$$q_B = \left[\frac{\partial k}{\partial z_D} + k \right]_{z=L} \quad (2.28)$$

Consider (2.27) again but rearranged to

$$q - k = \frac{\partial k}{\partial z_D} \quad (2.29)$$

then

$$\frac{\partial k}{q - k} = -\partial z_D \quad (2.30)$$

Taking the derivative

$$\ln(q - k) = -z_D + C \quad (2.31)$$

Simplifying and rearranging becomes

$$k = q - C e^{-z_D} \quad (2.32)$$

Applying the initial condition of $q = q_A$ and boundary condition of $k = e^{-a_k \psi_k}$ at

$z = 0$

$$e^{-a_k \psi_k} = q_A - C e^0 \quad (2.33)$$

gives

$$C = q_A - e^{-a_k \psi_k} \quad (2.34)$$

Finally, the expression for the initial condition is

$$k(z, 0) = q_A - (q_A - e^{-a_k \psi_k}) e^{-z_D} = k_0 \quad (2.35)$$

Therefore, the boundary and initial conditions are given by (2.22), (2.28), and (2.35).

2.5.1 PARTICULAR SOLUTION

With boundary and initial conditions already known, a particular and general solution to (2.21) will be obtained. First, the particular solution is simply $\frac{k_0}{p}$. Using

$$\bar{k}_1 = \frac{k_0}{p} = \frac{q_A}{p} - \frac{(q_A - e^{-a_k \psi_k}) e^{-z_D}}{p} \quad (2.36)$$

$$\frac{\partial \bar{k}}{\partial z_D} = (q_A - e^{-a_k \psi_k}) \frac{e^{-z_D}}{p} \quad (2.37)$$

$$\frac{\partial^2 \bar{k}}{\partial z_D^2} = -(q_A - e^{-a_k \psi_k}) \frac{e^{-z_D}}{p} \quad (2.38)$$

and substituting for (2.21)

$$\begin{aligned} & -(q_A - e^{-a_k \psi_k}) \frac{e^{-z_D}}{p} + (q_A - e^{-a_k \psi_k}) \frac{e^{-z_D}}{p} \\ & - d e^{\lambda z_D} [(q_A - e^{-a_k \psi_k}) e^{-z_D} - (q_A - e^{-a_k \psi_k}) e^{-z_D}] = 0 \end{aligned} \quad (2.39)$$

Therefore, $\bar{k}_1 = \frac{k_0}{p}$ is a particular solution of (2.21).

2.5.2 GENERAL SOLUTION

A general solution to (2.21) is found in chapter 2 of *Handbook of Integral Equations* (Polyanin and Zaitsev, 1995). For an equation of the form

$$y''_{xx} + ay'_x + (be^{\lambda x} + c)y = 0 \quad (2.40)$$

where a , b , and c are constant coefficients, the general solution is given by

$$y = e^{-\frac{ax}{2}} \left[C_1 J_\nu \left(\frac{2\sqrt{b}}{\lambda} e^{\frac{\lambda x}{2}} \right) + C_2 Y_\nu \left(\frac{2\sqrt{b}}{\lambda} e^{\frac{\lambda x}{2}} \right) \right] \quad (2.41)$$

where $\nu = \frac{\sqrt{a^2 - 4c}}{\lambda}$ and J_ν and Y_ν are Bessel functions.

Consider $\bar{k} = y$ and $z_D = x$, then letting $c = 0$ and $b = -d$ (2.40) will be in the form of (2.21). For simplicity, two new parameters will be introduced as C_1 and C_2 are being solved for.

$$\alpha = \frac{2\sqrt{-d}}{\lambda} \quad (2.42)$$

$$\beta = \frac{\lambda}{2} \quad (2.43)$$

where α and β are constants. The general solution is rewritten as

$$\bar{k}_2 = e^{-\frac{z_D}{2}} [C_1 J_\nu (\alpha e^{\beta z_D}) + C_2 Y_\nu (\alpha e^{\beta z_D})] \quad (2.44)$$

2.5.3 UNIQUE SOLUTION

The unique solution for (2.21) is therefore given by

$$\begin{aligned} \bar{k} = \bar{k}_1 + \bar{k}_2 = & \frac{q_A}{p} - \frac{(q_A - e^{-a_k \psi_k}) e^{-z_D}}{p} \\ & + e^{-\frac{z_D}{2}} [C_1 J_\nu(\alpha e^{\beta z_D}) + C_2 Y_\nu(\alpha e^{\beta z_D})] \end{aligned} \quad (2.45)$$

The boundary and initial conditions [(2.22), (2.28), and (2.35)] are applied to (2.45) to solve for the constants C_1 and C_2 . Taking the derivative of (2.45)

$$\begin{aligned} \frac{\partial \bar{k}}{\partial z_D} = & \frac{(q_A - e^{-a_k \psi_k}) e^{-z_D}}{p} - \left(\frac{e^{-\frac{z_D}{2}}}{2} \right) C_1 J_\nu(\alpha e^{\beta z_D}) \\ & + \alpha \beta e^{-\frac{z_D}{2}} C_1 J'_\nu(\alpha e^{\beta z_D}) - \left(\frac{e^{-\frac{z_D}{2}}}{2} \right) C_1 Y_\nu(\alpha e^{\beta z_D}) \\ & + \alpha \beta e^{-\frac{z_D}{2}} C_1 Y'_\nu(\alpha e^{\beta z_D}) \end{aligned} \quad (2.46)$$

where

$$J'_\nu = \frac{\partial J_\nu(z_D)}{\partial z_D} = \frac{\nu}{z_D} J_\nu(z_D) - J_{\nu+1}(z_D) \quad (2.47)$$

and

$$Y'_\nu = \frac{\partial Y_\nu(z_D)}{\partial z_D} = \frac{\nu}{z_D} Y_\nu(z_D) - Y_{\nu+1}(z_D) \quad (2.48)$$

From (2.22), for $z_D = 0$ $\bar{k} = \frac{e^{-a_k \psi_k}}{p}$

$$\frac{e^{-a_k \psi_k}}{p} = e^0 [C_1 J_\nu(\alpha e^0) + C_2 Y_\nu(\alpha e^0)] + \frac{q_A}{p} - \frac{(q_A - e^{-a_k \psi_k}) e^0}{p} \quad (2.49)$$

$$\frac{e^{-a_k \psi_k}}{p} = C_1 J_\nu(\alpha) + C_2 Y_\nu(\alpha) + \frac{q_A}{p} - \frac{q_A}{p} + \frac{e^{-a_k \psi_k}}{p} \quad (2.50)$$

$$C_1 J_\nu(\alpha) + C_2 Y_\nu(\alpha) = 0 \quad (2.51)$$

$$C_1 = -C_2 \left(\frac{Y_\nu(\alpha)}{J_\nu(\alpha)} \right) \quad (2.52)$$

Applying (2.28) to (2.45) and by substituting the expressions for \bar{k} and $\frac{\partial \bar{k}}{\partial z_D}$ at $z_D = L$

$$\begin{aligned} \frac{q_B}{p} &= e^{-\frac{L}{2}} [C_1 J_\nu(\alpha e^{\beta L}) + C_2 Y_\nu(\alpha e^{\beta L})] + \frac{q_A}{p} - \frac{(q_A - e^{-a_k \psi_k}) e^{-L}}{p} \quad (2.53) \\ &+ \frac{(q_A - e^{-a_k \psi_k}) e^{-L}}{p} - \frac{e^{-\frac{L}{2}}}{2} C_1 J_\nu(\alpha e^{\beta L}) + \alpha \beta e^{-\frac{L}{2}} C_1 J'_\nu(\alpha e^{\beta L}) \\ &- \frac{e^{-\frac{L}{2}}}{2} C_2 Y_\nu(\alpha e^{\beta L}) + \alpha \beta e^{-\frac{L}{2}} C_2 Y'_\nu(\alpha e^{\beta L}) \end{aligned}$$

Rearranging and simplifying gives

$$\begin{aligned} \frac{q_B - q_A}{p} &= \frac{e^{-\frac{L}{2}}}{2} C_1 J_\nu(\alpha e^{\beta L}) + \frac{e^{-\frac{L}{2}}}{2} C_2 Y_\nu(\alpha e^{\beta L}) \quad (2.54) \\ &+ \alpha \beta e^{-\frac{L}{2}} C_1 J'_\nu(\alpha e^{\beta L}) + \alpha \beta e^{-\frac{L}{2}} C_2 Y'_\nu(\alpha e^{\beta L}) \end{aligned}$$

Combining like terms

$$\begin{aligned} \frac{q_B - q_A}{p} &= C_1 \left[\frac{e^{-\frac{L}{2}}}{2} J_\nu(\alpha e^{\beta L}) + \alpha \beta e^{-\frac{L}{2}} J'_\nu(\alpha e^{\beta L}) \right] \quad (2.55) \\ &+ C_2 \left[\frac{e^{-\frac{L}{2}}}{2} Y_\nu(\alpha e^{\beta L}) + \alpha \beta e^{-\frac{L}{2}} Y'_\nu(\alpha e^{\beta L}) \right] \end{aligned}$$

Substituting for C_1

$$\begin{aligned} \frac{q_B - q_A}{p} &= -C_2 \left(\frac{Y_\nu(\alpha)}{J_\nu(\alpha)} \right) \left[\frac{e^{-\frac{L}{2}}}{2} J_\nu(\alpha e^{\beta L}) + \alpha \beta e^{-\frac{L}{2}} J'_\nu(\alpha e^{\beta L}) \right] \quad (2.56) \\ &+ C_2 \left[\frac{e^{-\frac{L}{2}}}{2} Y_\nu(\alpha e^{\beta L}) + \alpha \beta e^{-\frac{L}{2}} Y'_\nu(\alpha e^{\beta L}) \right] \end{aligned}$$

Solving for C_2 and letting

$$\Lambda = \left[\frac{e^{-\frac{L}{2}}}{2} Y_\nu(\alpha e^{\beta L}) + \alpha \beta e^{-\frac{L}{2}} Y'_\nu(\alpha e^{\beta L}) \right] - \frac{Y_\nu(\alpha)}{J_\nu(\alpha)} \left[\frac{e^{-\frac{L}{2}}}{2} J_\nu(\alpha e^{\beta L}) + \alpha \beta e^{-\frac{L}{2}} J'_\nu(\alpha e^{\beta L}) \right] \quad (2.57)$$

$$C_2 = \frac{q_B - q_A}{\Lambda} \quad (2.58)$$

and

$$F(p) = \frac{1}{p\Lambda} \quad (2.59)$$

C_2 becomes

$$C_2 = (q_B - q_A)F(p) \quad (2.60)$$

and

$$C_1 = -(q_B - q_A) \left(\frac{Y_\nu(\alpha)}{J_\nu(\alpha)} \right) F(p) \quad (2.61)$$

Replacing C_1 and C_2 in (2.45)

$$\begin{aligned} \bar{k} &= \frac{q_A}{p} - \frac{(q_A - e^{-a_k \psi_k}) e^{-zD}}{p} \\ &+ e^{-\frac{zD}{2}} \left[-(q_B - q_A) \left(\frac{Y_\nu(\alpha)}{J_\nu(\alpha)} \right) F(p) J_\nu(\alpha e^{\beta zD}) + (q_B - q_A) F(p) Y_\nu(\alpha e^{\beta zD}) \right] \end{aligned} \quad (2.62)$$

The unique solution to (2.45) is

$$\begin{aligned} \bar{k} &= \frac{q_A}{p} - \frac{(q_A - e^{-a_k \psi_k}) e^{-zD}}{p} \\ &+ e^{-\frac{zD}{2}} (q_B - q_A) F(p) \left[Y_\nu(\alpha e^{\beta zD}) - \left(\frac{Y_\nu(\alpha)}{J_\nu(\alpha)} \right) J_\nu(\alpha e^{\beta zD}) \right] \end{aligned} \quad (2.63)$$

Finally, equation (2.63) is the non-dimensional Laplace space solution to 1-D infiltration from the ground to the water table in single layer of homogeneous and isotropic soil. The procedure to invert equation (2.63) back into real space will be discussed in the following chapters using a modified numerical Laplace transform inversion MATLAB file (de Hoog et al., 1982).

CHAPTER 3

RESULTS AND DISCUSSION

3.1 INTRODUCTION

This chapter of thesis compares the proposed four parameter approach to the exponential representation of hydraulic parameters, K and θ with that of Srivastava and Yeh (1991) for time dependent conditions as a function of depth, z and pressure head, ψ . Furthermore, this chapter will validate the four parameter approach against the numerical solution of HYDRUS-1D, which is derived from the Van Genuchten (1980)-Mualem (1976) hydraulic model. This chapter will also demonstrate how to obtain van Genuchten parameters α and n using the developed solution. Finally, a comparison is shown between a fitted exponential representation of K and S_e to the van Genuchten-Mualem model.

3.2 COMPARISON WITH ANALYTICAL SOLUTION

This section will compare the proposed analytical solution discussed in chapter two to that of Srivastava and Yeh (1991). The system is defined in Figure 2.1 where the datum is set at the water table and positive upwards. As a boundary condition, pressure head at the water table is set to zero, $\psi_0 = 0 \text{ cm}$. The distance from the water table to the ground surface, L , is 100 cm and saturated hydraulic

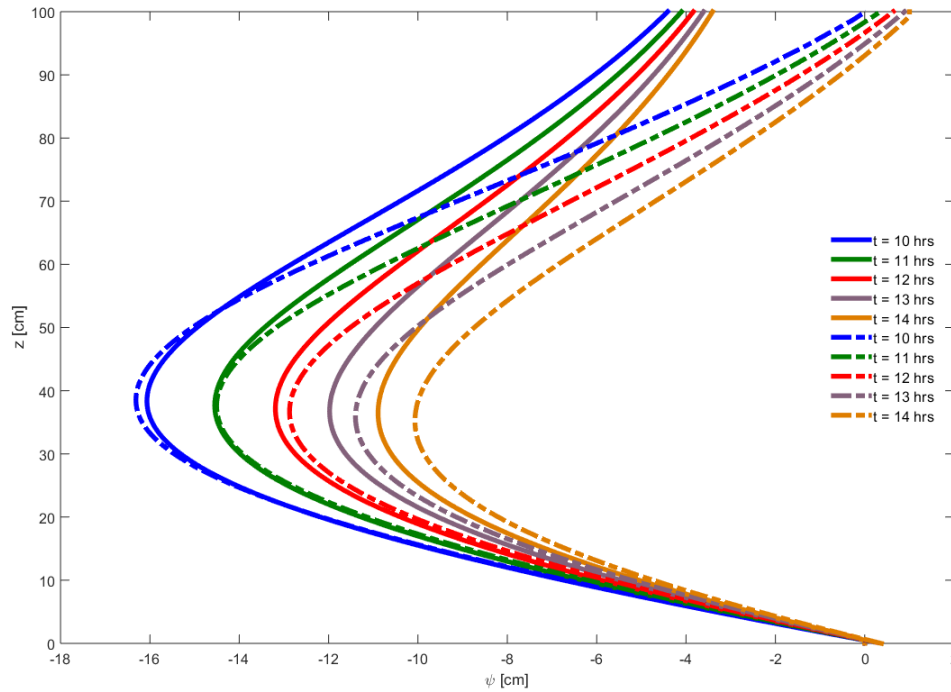


FIGURE 3.1: Wetting front: depth versus pressure head for $\psi_k = \psi_a = 1 \text{ cm}$, $a_k = 0.05 \text{ cm}^{-1}$ $a_c = 0.04 \text{ cm}^{-1}$ and $\alpha = 0.05 \text{ cm}^{-1}$.

θ_s	θ_r	$K_{sat}(\frac{cm}{hr})$
0.45	0.2	1

TABLE 3.1: Soil characteristics for Figures 3.1, 3.2, 3.3

θ_s	θ_r	$K_{sat}(\frac{cm}{hr})$
0.6	0.45	1

TABLE 3.2: Soil characteristics for Figures 3.5 and 3.4

conductivity, $K = 1 \text{ cm/hr}$ for each case. The rest of the soil parameters required for analysis using the Srivastava and Yeh (1991) and developed solution are found in Tables 3.1 and 3.2.

To use solution (2.63) developed in Chapter 2, one must use a computational software or program such as MATLAB, which will be used here.

3.2.1 LAPLACE INVERSION USING SOFTWARE PROGRAM

As discussed in Chapter 2, the solution to one dimensional vertical infiltration from the ground to the water table is described as equation (2.63). This solution, however, is in Laplace space and must be inverted back into real numbers. To do this a modified Laplace inversion MATLAB m-file developed by de Hoog et al. (1982) is employed. The Laplace inversion m-file requires inputs of t_D , t_{Dmax} , N_k , $params$, x , and z_D and passes along these parameters to the developed solution, equation (2.63). Finally, the Laplace inversion returns numerical values in real numbers for relative hydraulic conductivity, k . The values of k are then used to compute ψ and θ as a function of depth.

3.2.2 GRAPHICAL COMPARISON

A comparison of depth versus pressure head is seen in Figure 3.1 for time ranging between 10 and 14 hrs. The solid colored lines represent the solution given by Srivastava and Yeh (1991) and the dashed colored lines represent the developed solution in Figures 3.3, 3.1, and 3.2. Both solutions are passed along through the Laplace inversion in MATLAB discussed previously. Figure 3.1 illustrates the ability to calculate K as a function of depth during a storm event (wetting front). The curves furthest left represent time of 10 hrs and time increases by 1 hr as you move along each set of curves to the right. At the ground surface, $z = 100$ cm, water is entering and soil becomes more saturated with time. Alternatively, when

$q_B < q_A$ the situation becomes a drainage condition, seen in Figure 3.2. Both solutions indicate their ability to compute K as a function of depth and time.

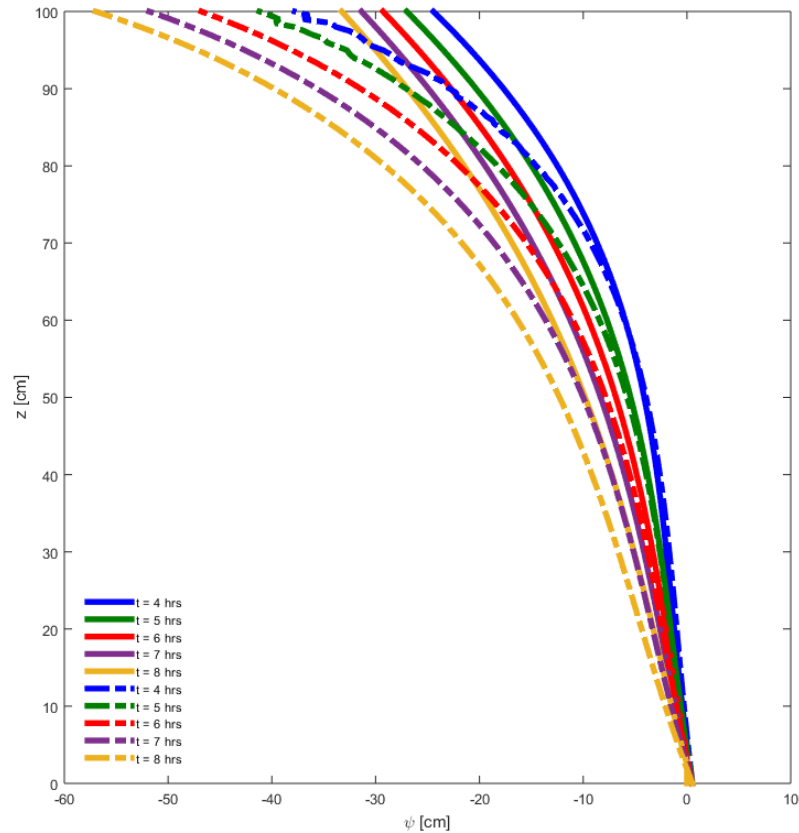


FIGURE 3.2: Drainage: depth versus pressure head for $\psi_k = \psi_a = 1 \text{ cm}$, $a_k = 0.035 \text{ cm}^{-1}$, $a_c = 0.025 \text{ cm}^{-1}$ and $\alpha = 0.035 \text{ cm}^{-1}$

The comparison of moisture profiles is seen in Figure 3.3. Both models illustrate the ability to compute water content, θ , as a function of pressure head, ψ . The curve shapes of Figures 3.1 and 3.3 are similar as a result of K and θ being expressed as exponential functions.

The effects of varying exponential parameters a_k and a_c are shown in Figures 3.5 and 3.4. For the same initial and boundary conditions of $q_A = 0.1 \text{ cm/hr}$,

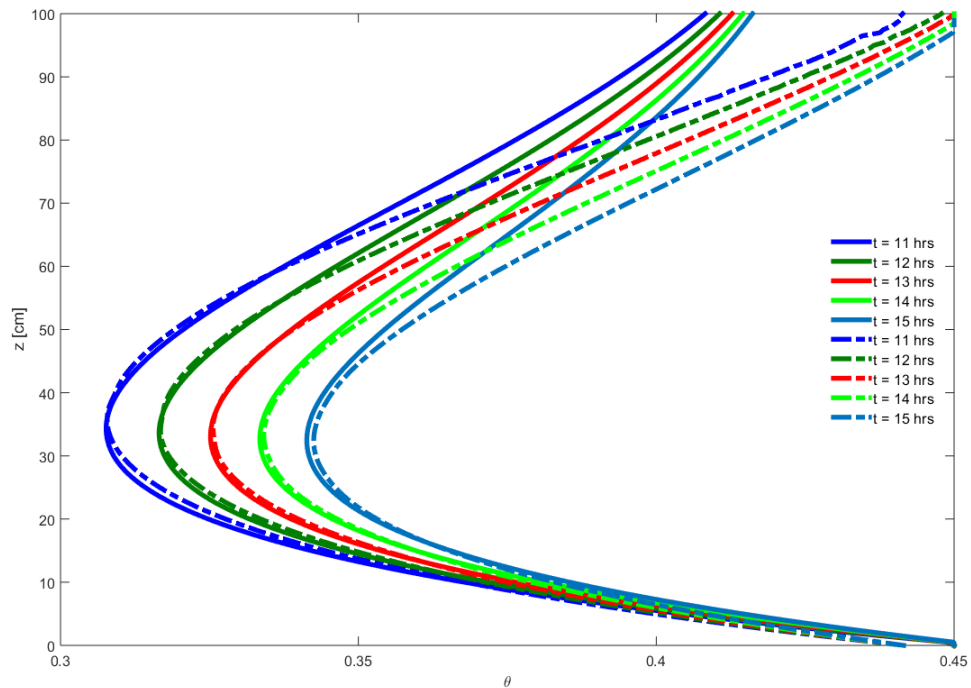


FIGURE 3.3: Depth versus water content for $\psi_k = \psi_a = 1 \text{ cm}$, $a_k = 0.06 \text{ cm}$, $a_c = 0.05 \text{ cm}$ and $\alpha = 0.06 \text{ cm}^{-1}$

$q_B = 0.9 \text{ cm/hr}$, and $\psi(0) = 0 \text{ cm}$, Figure 3.4 expresses K versus z with a fixed value of a_k at 0.04 cm^{-1} and a_c ranging from 0.06 to 0.1 cm^{-1} . Also noted, Figure 3.4 is for $t = 50 \text{ hrs}$. When keeping a_k constant, hydraulic conductivity drops consistently while a_c increases. As a_c approaches a_k the solution converges to that of Srivastava and Yeh (1991). By letting $a_c \neq a_k$ the solution expresses more flexibility in representing the system.

When a_c is fixed and a_k is allowed to be varied, the result is depicted in Figure 3.5. Again it is shown that K changes considerably as a result of varying a_k . Using previously published solutions would ignore the effects of varying a_k and would thus not encompass the system representation in its entirety. Again, when a_k approaches a_c the solution converges to the Srivastava and Yeh (1991) solution.

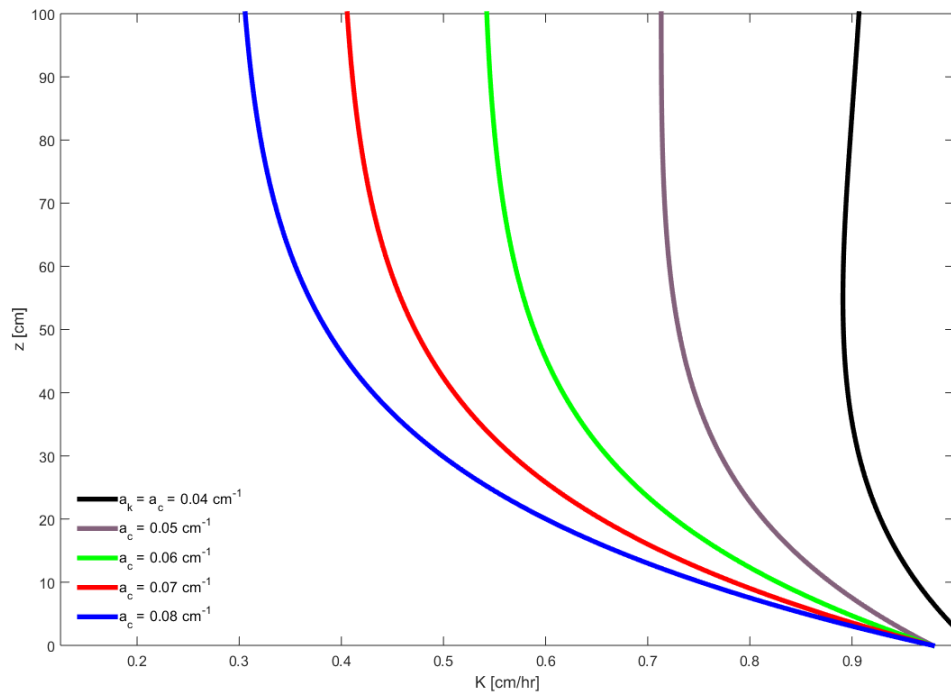


FIGURE 3.4: Depth versus hydraulic conductivity at $t = 50 \text{ hrs}$ when $\psi_k = \psi_a = 1 \text{ cm}^{-1}$

3.3 COMPARISON WITH NUMERICAL SOLUTION

This section presents a comparison of the developed solution to that of HYDRUS-1D for water infiltration. The HYDRUS-1D solution is obtained through the implementation of the Van Genuchten (1980)-Mualem (1976) model for unsaturated soils. The system is similar to that described previously and is seen in Figure 2.1. To achieve steady state in the HYDRUS software, the initial flux of $q_A = 0.1 \text{ cm/hr}$ is taken at time $t = 100 \text{ hrs}$ and the output is used as an initial condition for the increased flux of $q_B = 0.9 \text{ cm/hr}$. The remaining parameters used for the comparison are found in Table 3.3.

The parameters a_k , a_c , ψ_k , and ψ_a are determined using the least squares method

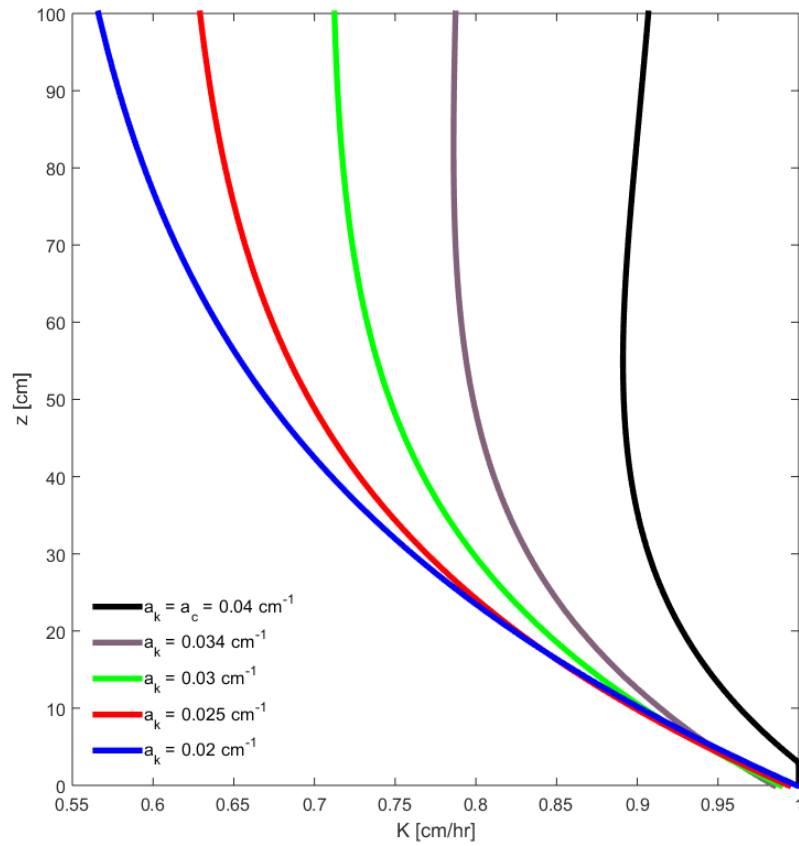


FIGURE 3.5: Depth versus hydraulic conductivity at $t = 50$ hrs when $\psi_k = \psi_a = 1 \text{ cm}^{-1}$

$q_A(\frac{cm}{hr})$	$q_B(\frac{cm}{hr})$	θ_s	θ_r
0.1	0.9	0.375	0.053
$K_{sat}(\frac{cm}{hr})$	$\alpha(\frac{1}{cm})$	n	
36	0.0416	2.4963	

TABLE 3.3: Soil characteristic inputs for HYDRUS-1D software

of MATLAB. A comparison using these obtained parameters with the HYDRUS simulation is seen in Figure 3.6.

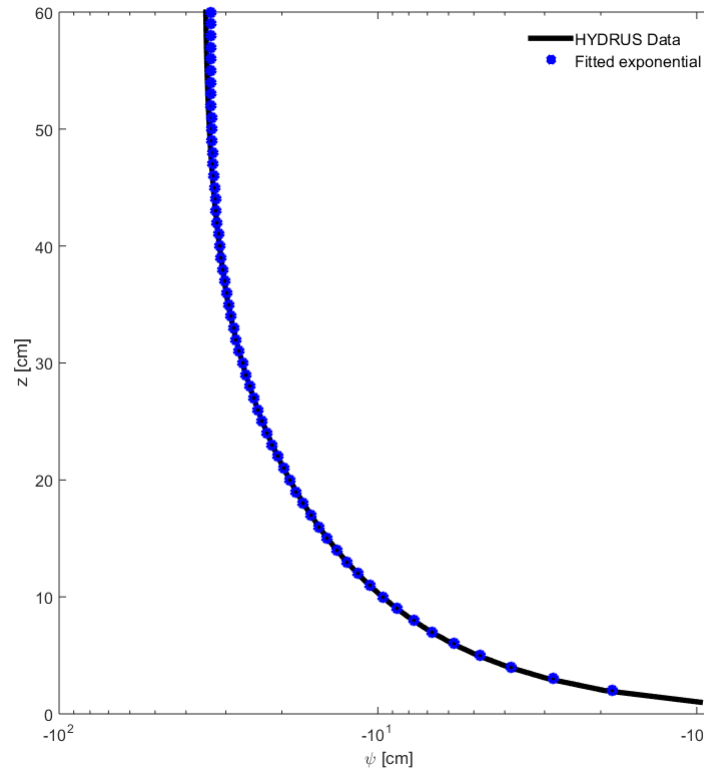


FIGURE 3.6: Depth versus pressure head for $t = 50 \text{ hrs}$ when $\psi_k = 5.4626 \text{ cm}$, $\psi_a = 9 \text{ cm}$, $a_k = 0.135 \text{ cm}^{-1}$, $a_c = 0.029 \text{ cm}^{-1}$, $\alpha = 0.0416 \text{ cm}^{-1}$, and $n = 2.4963$

3.4 DETERMINING VAN GENUCHTEN PARAMETERS AND COMPARISON OF EXPONENTIAL FUNCTIONS

Soil characteristics can be obtained through a variety of field or laboratory experiments, such as the ring infiltrometer, sprinkling infiltrometer, or vertical column infiltration experiments. The pressure head and water content can be measured from one of these processes and the proposed solution can be applied to this data using least squares best fit optimization to determine ψ_k , ψ_a , a_k , and a_c . This thesis uses HYDRUS-1D in lieu of field data to obtain the aforementioned four

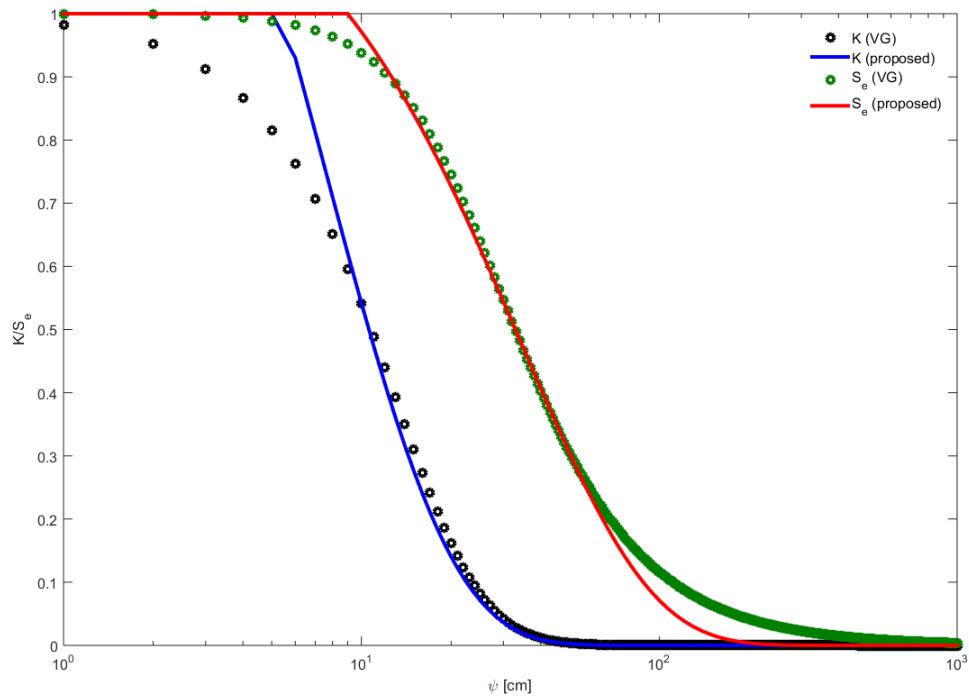


FIGURE 3.7: Depth versus pressure head for $\psi_k = 5.4626 \text{ cm}$, $\psi_a = 9.0 \text{ cm}$, $a_k = 0.135 \text{ cm}^{-1}$, $a_c = 0.029 \text{ cm}^{-1}$, $\alpha = 0.0416 \text{ cm}^{-1}$, and $n = 2.4963$

parameters. Next, one uses the expressions given by Ghezzehei et al. (2007)

$$\alpha \approx \frac{a_k}{1.3n} \quad (3.1)$$

and when $n > 2$,

$$\psi_k \approx \frac{1 - \left(\frac{n}{2}\right)^{-1.163}}{\alpha} \quad (3.2)$$

With values of $a_k = 0.135 \text{ cm}^{-1}$ and $\psi_k = 5.4626 \text{ cm}$ the corresponding values of α and n are therefore 0.0416 and 2.4963, respectively.

Lastly, the proposed model is further validated by fitting the relative hydraulic conductivity and effective saturation exponential functions to the Van Genuchten

(1980)-Mualem (1976) functions. Figure 3.7 shows the best fit representation discussed where $\alpha = 0.0416 \text{ cm}^{-1}$ and $n = 2.4963$ in (1.11) and (1.12) and $\psi_k = 5.4626 \text{ cm}$, $\psi_a = 9.0 \text{ cm}$, $a_k = 0.135 \text{ cm}^{-1}$, and $a_c = 0.029 \text{ cm}^{-1}$ in (2.63).

CHAPTER 4

CONCLUSION AND FUTURE SCOPE

4.1 CONCLUSION

Water infiltration in the vadose zone is an important aspect to the hydrologic cycle. Trees and other vegetation depend on the water from the vadose zone for nourishment. Additionally, soil characteristics are required for construction of buildings, such as soil pressure and water content, to name a few. Furthermore, in the case of soil remediation, hydraulic conductivity determines the rate at which a contaminated plume will flow through the soil.

This thesis establishes the following:

1. Determining van Genuchten parameters α and n can be cumbersome leading to dependence of parameter estimation techniques.
2. Beginning by representing hydraulic conductivity and water content as exponential functions dependent on pressure head then applying these to Richards' equation an analytical solution is developed for variably saturated soil. This unique approach utilizes four parameters (ψ_k , ψ_a , a_k , and a_c) first used by Mishra and Neuman (2010) to describe a wider range of soil conditions previously not represented using less parameters.

3. The developed solution is first compared to the published solution presented by Srivastava and Yeh (1991) for early and late time after initial infiltration. The solutions presented similar results as expected but the four parameter model expanded the possible outcomes of the system. Additionally, when $a_c = a_k$ the developed solution simplifies to the Srivastava and Yeh (1991) solution.
4. Another comparison of the developed solution is presented against HYDRUS-1D which uses the Van Genuchten (1980)-Mualem (1976) model to generate solutions of water infiltration. Using parameters of $a_k = 0.135 \text{ cm}^{-1}$, $a_c = 0.029 \text{ cm}^{-1}$, $\psi_k = 5.4626 \text{ cm}$, and $\psi_a = 9 \text{ cm}$ in the developed solution provided a best fit representation to the output generated by HYDRUS-1D, further validating the solution.
5. Finally, using the expression presented by Ghezzehei et al. (2007) one can determine van Genuchten parameters α and n when a_k and ψ_k are known. For the system setup and parameters used in the previous chapter, values of $a_k = 0.135 \text{ cm}^{-1}$ and $\psi_k = 5.4626 \text{ cm}$ yield van Genuchten parameters of $\alpha = 0.0416 \text{ cm}^{-1}$ and $n = 2.4963$.

4.2 FUTURE SCOPE

The proposed solution for vertical one dimensional infiltration considers a single homogeneous and isotropic layer of soil. To represent common conditions found at sites one must consider a multi-layer soil system. Future work to consider is to expand on the solution presented in this thesis to consider the multi-layered soil system where additionally boundary conditions are required but can be obtained

from continuity of flux and pressure at soil boundaries. Additional work to consider is comparing the developed solution with field data and/or laboratory experiments of single layered soil infiltration.

APPENDIX

HYDRUS-1D AND FITTED MODEL OUTPUTS

TABLE A.1: HYDRUS-1D Simulated Data

Elevation Head z (cm)	Pressure Head ψ (cm)	Water Content θ	Hydraulic Conductivity K (cm/hr)
0	-35.065	0.2045	9.00E-01
-1	-35.065	0.2045	9.01E-01
-2	-35.063	0.2045	9.02E-01
-3	-35.062	0.2046	9.03E-01
-4	-35.059	0.2046	9.03E-01
-5	-35.056	0.2046	9.04E-01
-6	-35.052	0.2046	9.05E-01
-7	-35.048	0.2046	9.05E-01
-8	-35.043	0.2046	9.06E-01
-9	-35.038	0.2046	9.06E-01
-10	-35.033	0.2047	9.07E-01
-11	-35.027	0.2047	9.07E-01
-12	-35.021	0.2047	9.07E-01
-13	-35.014	0.2047	9.08E-01
-14	-35.008	0.2048	9.08E-01
-15	-35.002	0.2048	9.08E-01
-16	-34.995	0.2048	9.08E-01
-17	-34.989	0.2048	9.07E-01
-18	-34.983	0.2049	9.07E-01
-19	-34.976	0.2049	9.07E-01
-20	-34.97	0.2049	9.07E-01
-21	-34.964	0.205	9.07E-01
-22	-34.958	0.205	9.07E-01
-23	-34.951	0.205	9.07E-01
-24	-34.945	0.205	9.07E-01
-25	-34.938	0.2051	9.07E-01
-26	-34.931	0.2051	9.07E-01
-27	-34.924	0.2052	9.07E-01

continued ...

... continued

Elevation Head z (cm)	Pressure Head ψ (cm)	Water Content θ	Hydraulic Conductivity K (cm/hr)
-28	-34.915	0.2052	9.08E-01
-29	-34.906	0.2052	9.09E-01
-30	-34.896	0.2053	9.10E-01
-31	-34.884	0.2054	9.11E-01
-32	-34.871	0.2054	9.12E-01
-33	-34.856	0.2055	9.14E-01
-34	-34.838	0.2056	9.16E-01
-35	-34.818	0.2057	9.19E-01
-36	-34.795	0.2058	9.22E-01
-37	-34.767	0.2059	9.26E-01
-38	-34.736	0.2061	9.30E-01
-39	-34.7	0.2063	9.35E-01
-40	-34.658	0.2065	9.40E-01
-41	-34.611	0.2067	9.47E-01
-42	-34.556	0.207	9.54E-01
-43	-34.494	0.2073	9.62E-01
-44	-34.423	0.2076	9.71E-01
-45	-34.343	0.208	9.82E-01
-46	-34.253	0.2085	9.93E-01
-47	-34.152	0.209	1.01E+00
-48	-34.038	0.2095	1.02E+00
-49	-33.911	0.2101	1.04E+00
-50	-33.77	0.2108	1.06E+00
-51	-33.614	0.2116	1.07E+00
-52	-33.441	0.2124	1.10E+00
-53	-33.252	0.2133	1.12E+00
-54	-33.045	0.2143	1.15E+00
-55	-32.82	0.2154	1.17E+00
-56	-32.575	0.2166	1.21E+00
-57	-32.311	0.2179	1.24E+00
-58	-32.026	0.2193	1.27E+00
-59	-31.722	0.2208	1.31E+00
-60	-31.396	0.2224	1.35E+00
-61	-31.051	0.2241	1.40E+00
-62	-30.685	0.2258	1.44E+00
-63	-30.298	0.2277	1.49E+00

continued ...

... continued

Elevation Head z (cm)	Pressure Head ψ (cm)	Water Content θ	Hydraulic Conductivity K (cm/hr)
-64	-29.892	0.2297	1.54E+00
-65	-29.451	0.2323	1.67E+00
-66	-28.964	0.2353	1.83E+00
-67	-28.433	0.2386	2.01E+00
-68	-27.861	0.2421	2.19E+00
-69	-27.254	0.2459	2.39E+00
-70	-26.614	0.2498	2.60E+00
-71	-25.946	0.2539	2.82E+00
-72	-25.253	0.2582	3.04E+00
-73	-24.538	0.2626	3.28E+00
-74	-23.802	0.2672	3.52E+00
-75	-23.042	0.2723	3.98E+00
-76	-22.254	0.2777	4.52E+00
-77	-21.441	0.2833	5.07E+00
-78	-20.609	0.289	5.64E+00
-79	-19.761	0.2948	6.22E+00
-80	-18.899	0.3008	6.81E+00
-81	-18.022	0.3067	7.74E+00
-82	-17.131	0.3127	8.76E+00
-83	-16.228	0.3188	9.79E+00
-84	-15.315	0.3249	1.08E+01
-85	-14.394	0.3308	1.21E+01
-86	-13.464	0.3363	1.36E+01
-87	-12.527	0.3419	1.50E+01
-88	-11.584	0.3472	1.66E+01
-89	-10.635	0.3518	1.83E+01
-90	-9.682	0.3564	2.01E+01
-91	-8.725	0.3603	2.20E+01
-92	-7.764	0.3639	2.39E+01
-93	-6.8	0.3669	2.58E+01
-94	-5.833	0.3695	2.78E+01
-95	-4.865	0.3714	2.96E+01
-96	-3.894	0.3729	3.13E+01
-97	-2.922	0.374	3.30E+01
-98	-1.949	0.3746	3.43E+01
-99	-0.975	0.3749	3.54E+01

continued ...

... continued

Elevation Head z (cm)	Pressure Head ψ (cm)	Water Content θ	Hydraulic Conductivity K (cm/hr)
-100	0	0.375	3.60E+01

TABLE A.2: MATLAB Data

Elevation Head z (cm)	Pressure Head ψ (cm)	Hydraulic Conductivity K (cm/hr)
100	-17.08290982	1.715792568
99	-17.5990896	1.600299568
98	-18.19459501	1.4766819
97	-18.85647629	1.350457792
96	-19.57192486	1.226124133
95	-20.32217274	1.108019977
94	-21.09957777	0.997627757
93	-21.89877002	0.895595862
92	-22.69802708	0.803992195
91	-23.48949355	0.722517462
90	-24.26585996	0.650624143
89	-25.02080049	0.587581612
88	-25.74901499	0.532565659
87	-26.44511835	0.484797966
86	-27.09629233	0.44399964
85	-27.70789923	0.408812584
84	-28.29026503	0.377902958
83	-28.831715	0.35126527
82	-29.33229273	0.328311778
81	-29.7927086	0.308526444
80	-30.21360598	0.291484377
79	-30.59576084	0.276827759
78	-30.94114087	0.264216594
77	-31.25393531	0.253291741
76	-31.53881409	0.243735425
75	-31.79859335	0.235335726
74	-32.03484361	0.22794841
73	-32.24906634	0.221450539
72	-32.44290451	0.215730751
71	-32.61793494	0.210692979
70	-32.77545574	0.206259832
69	-32.91637486	0.202373016
68	-33.04123603	0.198990354
67	-33.1503835	0.196079746
66	-33.244199	0.193612038
65	-33.32329173	0.19155574

continued ...

... continued

Elevation Head z (cm)	Pressure Head ψ (cm)	Hydraulic Conductivity K (cm/hr)
64	-33.38855022	0.189875565
63	-33.44105453	0.18853447
62	-33.48191791	0.187497273
61	-33.51213358	0.186734007
60	-33.53246691	0.186222125
59	-33.54340119	0.185947441
58	-33.54513518	0.185903918
57	-33.53763807	0.186092168
56	-33.52075885	0.186516699
55	-33.49432912	0.187183381
54	-33.45814469	0.18809999
53	-33.41181549	0.189280137
52	-33.35464485	0.190746661
51	-33.28564629	0.19253173
50	-33.20363477	0.194675199
49	-33.10730189	0.197223472
48	-32.99525223	0.200229491
47	-32.86601658	0.20375351
46	-32.71805859	0.207864268
45	-32.54978366	0.212640389
44	-32.35955308	0.218171958
43	-32.14570442	0.224562288
42	-31.90657783	0.231929909
41	-31.64054789	0.24041083
40	-31.34606004	0.2501611
39	-31.02167021	0.261359731
38	-30.66608598	0.274212022
37	-30.27820697	0.288953356
36	-29.85716217	0.305853529
35	-29.40234165	0.325221697
34	-28.91342031	0.347412028
33	-28.39037195	0.372830169
32	-27.83347244	0.401940649
31	-27.24329178	0.435275354
30	-26.62067566	0.473443227
29	-25.96671786	0.517141383
28	-25.28272559	0.567167833

continued ...

... continued

Elevation Head z (cm)	Pressure Head ψ (cm)	Hydraulic Conductivity K (cm/hr)
27	-24.57018	0.624436047
26	-23.83069445	0.68999163
25	-23.06597275	0.765031414
24	-22.27776939	0.850925304
23	-21.4678533	0.949241289
22	-20.63797618	1.061774064
21	-19.789846	1.190577792
20	-18.9251058	1.338003604
19	-18.04531774	1.506742512
18	-17.15195181	1.699874533
17	-16.24637885	1.92092491
16	-15.32986711	2.173928455
15	-14.40358174	2.463503203
14	-13.46858664	2.794934697
13	-12.52584796	3.174272473
12	-11.57623897	3.608440475
11	-10.62054566	4.105363438
10	-9.659472883	4.674111538
9	-8.693650687	5.325065946
8	-7.723640661	6.070108315
7	-6.749942134	6.922837648
6	-5.772998103	7.898818525
5	-4.793200846	9.015865189
4	-3.81089714	10.29436671
3	-2.826393095	11.75765915
2	-1.839958572	13.43245148
1	-0.85183121	15.34931312
0	0	17.54323191

BIBLIOGRAPHY

- Almedeij, J. and Esen, I. (2013). Modified green-ampt infiltration model for steady rainfall. *Journal of Hydrologic Engineering*, 19(9):04014011.
- Bouwer, H. (1966). Rapid field measurement of air entry value and hydraulic conductivity of soil as significant parameters in flow system analysis. *Water Resources Research*, 2(4):729–738.
- Darcy, H. (1856). Les fontaines publiques de la ville de Dijon. *Dalmont, Paris*, 647.
- de Hoog, F., Knight, J., and Stokes, A. (1982). An improved method for numerical inversion of laplace transforms. *SIAM Journal on Scientific and Statistical Computing*, 3:357.
- Gardner, W. (1958). Some steady-state solutions of the unsaturated moisture flow equation with application to evaporation from a water table. *Soil Science*, 85(4):228.
- Ghezzehei, T. A., Kneafsey, T. J., and Su, G. W. (2007). Correspondence of the gardner and van genuchten–mualem relative permeability function parameters. *Water Resources Research*, 43(10).
- Green, W. H. and Ampt, G. (1911). Studies on soil physics, 1. the flow of air and water through soils. *Journal of Agricultural Science*, 4(1):1–24.
- Herrada, M. A., Gutiérrez-Martin, A., and Montanero, J. M. (2014). Modeling infiltration rates in a saturated/unsaturated soil under the free draining condition. *Journal of Hydrology*, 515:10–15.
- Horton, R. E. (1933). The role of infiltration in the hydrologic cycle. *Eos, Transactions American Geophysical Union*, 14(1):446–460.
- Ma, Y., Feng, S., Zhan, H., Liu, X., Su, D., Kang, S., and Song, X. (2010). Water infiltration in layered soils with air entrapment: modified green-ampt model and experimental validation. *Journal of Hydrologic Engineering*, 16(8):628–638.
- Mein, R. G. and Larso, C. L. (1973). Modelling soil water dynamics in the unsaturated zonestate of the art. *Water Resources Research*, 9:384–394.

- Mishra, P. and Neuman, S. (2010). Improved forward and inverse analyses of saturated-unsaturated flow toward a well in a compressible unconfined aquifer. *Water Resources Research*, 46(7):W07508.
- Mishra, P. and Neuman, S. (2011). Saturated-unsaturated flow toward a well with storage in a compressible unconfined aquifer. *Water Resources Research*, 47(7):W12508.
- Mualem, Y. (1976). A new model for predicting the hydraulic conductivity of unsaturated porous media. *Water Resources Research*, 12(3):513–522.
- Philip, J. (1958). The theory of infiltration: 6 effect of water depth over soil. *Soil Science*, 85(5):278–286.
- Polyanin, A. D. and Zaitsev, V. F. (1995). Handbook of exact solutions for ordinary differential equations. *CRC Press*, 1.
- Richards, L. A. (1931). Capillary conduction of liquids through porous mediums. *Journal of Applied Physics*, 1(5):318–333.
- Srivastava, R. and Yeh, T.-C. J. (1991). Analytical solutions for one-dimensional, transient infiltration toward the water table in homogeneous and layered soils. *Water Resources Research*, 27(5):753–762.
- Van Genuchten, M. T. (1980). A closed-form equation for predicting the hydraulic conductivity of unsaturated soils. *Soil Science Society of America Journal*, 44(5):892–898.